

# Ideal-Gas Heat Capacity for 2,3,3,3-Tetrafluoropropene (HFO-1234yf) Determined from Speed-of-Sound Measurements

Yuya Kano · Yohei Kayukawa · Kenichi Fujii ·  
Haruki Sato

Received: 2 August 2010 / Accepted: 10 November 2010 / Published online: 28 November 2010  
© Springer Science+Business Media, LLC 2010

**Abstract** The isobaric ideal-gas heat capacity for HFO-1234yf, which is expected to be one of the best alternative refrigerants for HFC-134a, was determined on the basis of speed-of-sound measurements in the gaseous phase. The speed of sound was measured by means of the acoustic resonance method using a spherical cavity. The resonance frequency in the spherical cavity containing the sample gas was measured to determine the speed of sound. After correcting for some effects such as the thermal boundary layer and deformation of the cavity on the resonance frequency, the speed of sound was obtained with a relative uncertainty of 0.01 %. Using the measured speed-of-sound data, the acoustic-virial equation was formulated and the isobaric ideal-gas heat capacity was determined with a relative uncertainty of 0.1 %. A temperature correlation function of the isobaric ideal-gas heat capacity for HFO-1234yf was also developed.

**Keywords** Acoustic resonance · HFO-1234yf (1,1,1,2-tetrafluoroethane) · Ideal-gas heat capacity · Speed of sound · Spherical resonator

## 1 Introduction

In Europe, the use of HFC-134a (1,1,1,2-tetrafluoroethane) in motor vehicle air-conditioning systems will phase down from the beginning of 2011 due to concerns

Y. Kano (✉) · Y. Kayukawa · K. Fujii  
Fluid Properties Section, Material Properties and Metrological Statistics Division, National Metrology Institute of Japan, National Institute of Advanced Industrial Science and Technology, AIST Tsukuba Central 3, 1-1-1 Umezono, Tsukuba, Ibaraki 305-8563, Japan  
e-mail: yuya-kano@aist.go.jp

H. Sato  
School of Science for Open and Environmental Systems, Keio University,  
3-14-1, Hiyoshi, Kohoku-ku, Yokohama 223-8522, Japan

about serious climate changes resulting from global warming. Currently, HFO-1234yf (2,3,3,3-tetrafluoropropene) is recognized as the strongest alternative candidate for HFC-134a [1]. The global warming potential (GWP) of HFO-1234yf is estimated to be about 4, which is much smaller than that of HFC-134a, being 1300. Thermophysical properties of HFO-1234yf, however, are not well known presently.

Thermophysical properties of refrigerants are vital information to realize efficient thermal energy conversion systems. In order to develop the thermodynamic equation of state providing some useful caloric properties such as enthalpy or entropy, information on the ideal-gas heat capacity is a necessity. Speed-of-sound measurements represent one of the best approaches to understand the thermodynamic behavior of dilute gases and to derive the ideal-gas heat capacity. Therefore, in the present study, the speed of sound in the gaseous phase for HFO-1234yf was measured on the basis of the acoustic resonance method with a spherical cavity. The isobaric ideal-gas heat capacity has been obtained from the measured speed-of-sound data.

## 2 Method for Speed-of-Sound Measurement

As details of the experimental apparatus and measurement procedure were already reported in previous papers [2–7], only a brief explanation for the speed-of-sound measurement system is given here. As illustrated in Fig. 1, a spherical resonator is placed in a pressure vessel, and the vessel is immersed in water whose temperature is controlled in a thermostatic bath. The sample gas is introduced into both the resonator and the vessel so that the pressures inside and outside the resonator are approximately equal. Thus, the inner volume of the resonator depends only on temperature. Both the resonator and the vessel are made of stainless steel (SUS304). The inner diameter of the resonator is about 100 mm, and the roughness and asphericity of the inner surface are manufactured within 50  $\mu\text{m}$  in total.

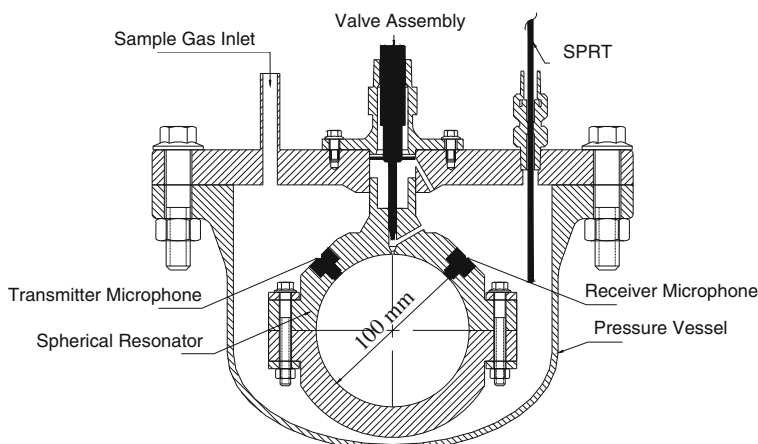


**Fig. 1** Cross-sectional view of the spherical resonator and pressure vessel; SPRT standard platinum resistance thermometer

Figure 2 shows a schematic diagram of the apparatus including the spherical resonator and thermostatic bath. The temperature fluctuations in the bath are controlled within 1 mK by using a standard platinum resistance thermometer (SPRT) and a PID control system. The temperature in the pressure vessel is also measured by another SPRT to observe the temperature fluctuation of the sample gas. Both SPRTs have been calibrated on the basis of ITS-90 [8]. The sample pressure is directly measured by a digital quartz pressure gauge placed outside the thermostatic bath.

The speed of sound,  $w$ , is determined from the measured values of the resonance frequency in the radially symmetric modes,  $f_{0,n}$ . A condenser microphone transmits the audio frequency sound signal into the resonator. The sound wave propagating in the sample gas is detected by another condenser microphone, and its amplifier and phase shift are measured with a lock-in amplifier. The frequency of the sound wave is scanned by using a frequency synthesizer so that the resonant frequency is obtained from the response curve. The relation between  $w$  and  $f_{0,n}$  is described in detail by Moldover et al. [9] as follows:

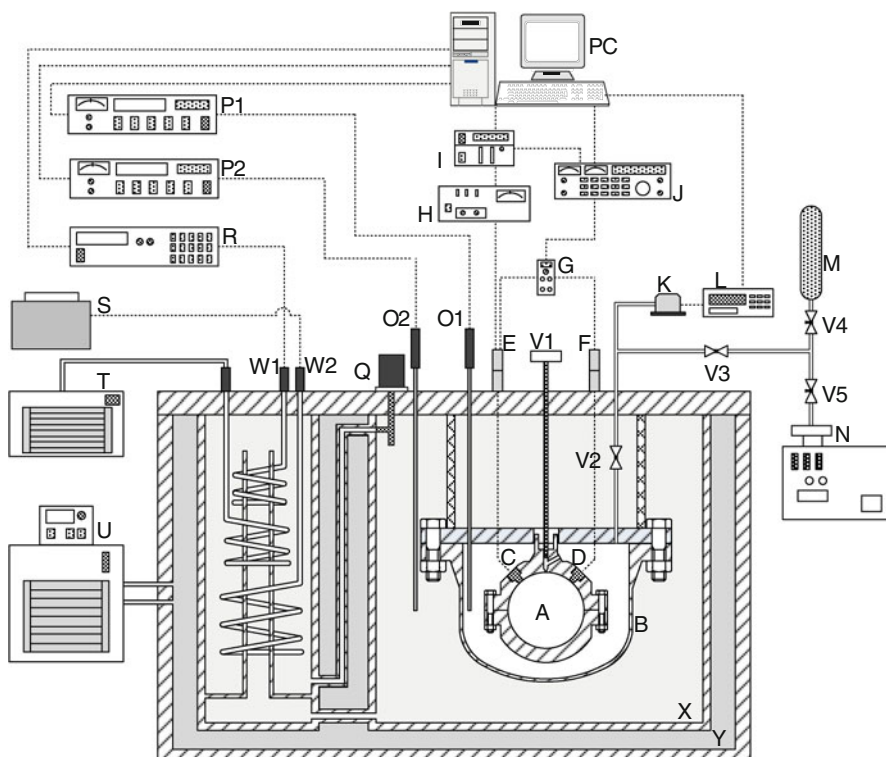


**Fig. 2** Schematic diagram of the experimental apparatus; A spherical resonator, B pressure vessel, C transmitter microphone, D detector microphone, E transmitter adapter, F preamplifier, G microphone power supply, H power amplifier, I frequency synthesizer, J lock in amplifier, K quartz pressure transducer, L digital pressure computer, M sample bomb, N vacuum pump, O1-2 standard platinum resistance thermometers, P1-2 thermometer bridges, Q circulator pump, R programmable power supply, S manual voltage controller, T cooler, U circular type thermostat, V1-5 valves, W1-2 heating coils, X internal thermostat, Y external prethermostat

$$f_{0,n} = \frac{wZ_{0,n}}{2\pi a} + \sum_j \Delta f_j. \quad (n = 0, 1, 2, \dots)$$
(1)

In Eq. 1, the parameter  $a$  denotes the inner radius of the spherical resonator, which is determined in advance by measuring the speed of sound in argon, and the parameter  $Z_{0,n}$  indicates the  $n$ -th root of the equation  $dj_0(z)/dz = 0$ , where  $j_0(z)$  is the zeroth order of the spherical Bessel function. The second term on the right-hand side of Eq. 1 is a series of perturbation terms to compensate for various non-ideal conditions in the acoustic resonance that has been carefully discussed by Mehl and Moldover [10] or Ewing et al. [11]. In this work, the effects of the thermal boundary layer and deformation of the spherical cavity were taken into account for correcting the resonance frequency. Other effects such as shell motion are vanishingly small.

The effect of the thermal boundary layer is given by

$$\Delta f_{\text{th}} = -\frac{\gamma - 1}{2a} \sqrt{\frac{D_t f_{0,n}}{\pi}} + (\gamma - 1) \frac{f_{0,n} l_a}{a},$$
(2)

where  $\gamma$ ,  $D_t$ , and  $l_a$  indicate the heat capacity ratio, thermal diffusivity, and thermal accommodation length, respectively. The second term on the right-hand side of Eq. 2 represents the temperature-jump effect, and  $l_a$  is defined as

$$l_a = \frac{\lambda}{p} \sqrt{\frac{\pi M T}{2R}} \frac{(2-h)/h}{c_v/R + 1/2},$$
(3)

where  $p$ ,  $\lambda$ ,  $R$ ,  $M$ ,  $T$ ,  $c_v$ , and  $h$  are the pressure, thermal conductivity, gas constant, molar mass, temperature, isochoric specific heat capacity, and thermal accommodation coefficient, respectively. The value of  $h$  is designated as unity in the present study.

Based on the theory discussed by Mehl [12], the effect of deformation of the spherical cavity on the resonant frequency is expressed as follows:

$$\Delta f_d = C_n \xi^2 f_{0,n}. \quad (n = 0, 1, 2, \dots)$$
(4)

The values of  $C_n$  from  $n = 1$  to 5 are given in Ref. [12]. However, we noticed that the correction for the (0, 1) mode is too large due to the (3, 1) mode lying only about 0.5 % above the frequency of the (0, 1) mode. Thus, we ignored the correction shown in Eq. 4 for the (0, 1) mode. The parameter of  $\xi$  was determined as  $6.39631 \times 10^{-3}$  by measuring argon so that standard deviations of the measured speed-of-sound data from the (0, 1) to (0, 5) modes are minimized.

### 3 Results for Speed-of-Sound Measurements

A sample of HFO-1234yf was obtained from SynQuest Laboratories Ltd. The purity of 99.9 % (determined by gas chromatography) for HFO-1234yf is claimed by the manufacturer. No further purification except degassing was conducted. In much the same way as described in previous papers [5, 6], an expanded relative uncertainty ( $k = 2$ )

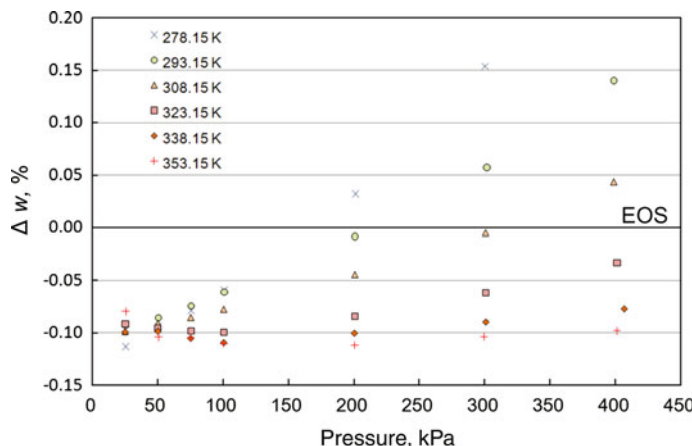


**Fig. 3** Deviations of the speed-of-sound measurements from the equation of state developed by Akasaka et al. [14]

for the speed-of-sound measurements is estimated on the basis of the ISO guideline [13] as 0.01 %. Similarly, expanded uncertainties for temperature and pressure measurements are estimated to be 4 mK and 0.1 kPa, respectively. The speed of sound was measured on each isotherm from 278.15 K up to 353.15 K and at pressures from 400 kPa down to 25 kPa. Average values of the (0, 1) to (0, 5) modes were used for determination of the speed-of-sound data. Thermophysical properties of HFO-1234yf in Eqs. 2 and 3 are estimated by using the equation of state developed by Akasaka et al. [14] for the equilibrium properties, and the extended corresponding-states model developed by Huber et al. [15] for the transport properties.

The numerical data for the speed of sound for HFO1234yf is tabulated in Table 1. Figure 3 also shows deviations of the speed-of-sound measurements from the equation of state developed by Akasaka et al. [14]. As shown in Fig. 3, almost all of the measured data agree well with the equation of state within a relative difference of 0.15 %, although no speed-of-sound data for HFO-1234yf were used for developing the equation. However, large discrepancies beyond the measurement uncertainty can be seen in Fig. 3. Thus, these speed-of-sound data should be used for improving the equation of state for HFO-1234yf.

#### 4 Ideal-Gas Heat Capacity for HFO-1234yf

The measured speed-of-sound data shown in Table 1 are correlated along each isotherm with the following acoustic-virial equation:

$$w^2 = \frac{\gamma^0}{M} \left( RT + \beta_a p + \gamma_a p^2 \right), \quad (5)$$

where  $\gamma^0$ ,  $\beta_a$ , and  $\gamma_a$  denote the ideal-gas heat capacity ratio, the second acoustic-virial coefficient, and the third acoustic-virial coefficient, respectively. The value of  $\gamma^0$  is

**Table 1** Speed-of-sound data for HFO-1234yf

<i>T</i> (K)	<i>P</i> (kPa)	<i>w</i> (m · s <sup>-1</sup> )	<i>T</i> (K)	<i>P</i> (kPa)	<i>w</i> (m · s <sup>-1</sup> )
278.150	25.443	148.085	323.150	25.338	159.311
278.150	50.618	147.246	323.150	50.233	158.760
278.150	75.677	146.389	323.150	75.473	158.200
278.150	100.999	145.514	323.150	100.590	157.639
278.150	201.302	141.892	323.150	200.868	155.386
278.150	300.476	138.019	323.150	300.933	153.067
293.150	25.293	151.927	323.150	401.339	150.657
293.150	50.994	151.191	338.150	25.366	162.835
293.150	75.571	150.473	338.150	50.452	162.357
293.150	101.227	149.719	338.150	75.499	161.866
293.150	201.078	146.669	338.151	100.773	161.371
293.150	292.415	143.725	338.150	200.631	159.424
293.150	401.237	139.994	338.150	301.182	157.410
308.150	25.257	155.675	338.150	407.009	155.227
308.150	50.393	155.053	353.149	25.671	166.316
308.150	75.504	154.421	353.151	50.667	165.858
308.150	100.641	153.786	353.151	75.382	165.441
308.150	200.865	151.183	353.151	100.553	165.006
308.150	300.848	148.470	353.152	200.638	163.292
308.150	398.917	145.683	353.147	299.528	161.574
			353.150	401.296	159.763

**Table 2** Isobaric ideal-gas heat capacity for HFO-1234yf

<i>T</i> (K)	<i>c</i> <sub><i>p</i></sub> <sup>0</sup> (J · mol <sup>-1</sup> · K <sup>-1</sup> )
278.150	97.239
293.150	100.595
308.150	103.577
323.150	106.583
338.150	109.895
353.150	112.598

obtained by linearly fitting Eq. 5 to the speed-of-sound data on each isotherm; then the isobaric ideal-gas heat capacity,  $c_p^0$ , is derived from the following relation:

$$\frac{c_p^0}{R} = \frac{\gamma^0}{\gamma^0 - 1}. \quad (6)$$

Through the above procedure, the value of  $c_p^0$  is determined as shown in Table 2 with a relative expanded uncertainty ( $k = 2$ ) of 0.1 %.

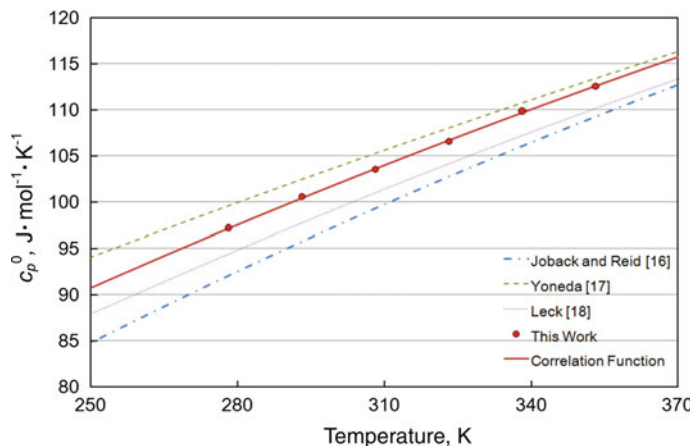


**Fig. 4** Comparison of the determined  $c_p^0$  values with some estimated values

Figure 4 shows a comparison of the determined  $c_p^0$  values with some estimated values, which are calculated on the basis of the atomic-group contribution methods developed by Joback and Reid [16], Yoneda [17], and a polynomial approximation reported by Leck [18] that is used for the equation of state for HFO-1234yf developed by Akasaka et al. [14]. The maximum deviations of the estimated values of  $c_p^0$  from the present work in a range of 250 K to 370 K, which is the valid range for the equation of state by Akasaka et al. [14], are  $-6.5\%$  for Joback and Reid [16],  $+3.6\%$  for Yoneda [17], and  $-3.1\%$  for Leck [18]. A difference of the order of several percent for  $c_p^0$  may lead to a wrong coefficient of performance (COP) estimation for the air-conditioning system in practical use. Since we believe our determined  $c_p^0$  values are the most reliable data for the present, the following temperature correlation function of  $c_p^0$  for HFO-1234yf was developed:

$$c_p^0 = \sum_{i=0}^3 c_i \left( \frac{T}{T_c} \right)^i. \quad (7)$$

In Eq. 7,  $T_c$  represents the critical temperature of HFO-1234yf, i.e., 367.85 K [19], and the fitted values of  $c_i$  ( $i: 0$  to 3) are shown in Table 3. The temperature correlation function of Eq. 7 reproduces the  $c_p^0$  values shown in Table 2 within a relative difference

**Table 3** Values of  $c_i$  in Eq. 7

$i$	$c_i (J \cdot mol^{-1} \cdot K^{-1})$
0	18.349
1	128.316
2	-33.354
3	2.086

of 0.15 %. This new  $c_p^0$  function will help improve the existing equation of state for HFO-1234yf.

## 5 Conclusion

In this study, the speed of sound in the gaseous phase of HFO-1234yf was measured by using a spherical acoustic resonator. As a result, 41 data for the speed of sound were obtained in the range of 278.15 K to 353.15 K with an expanded relative uncertainty of 0.01 %. Almost all of the speed-of-sound data agree with the existing equation of state within a relative difference of 0.15 %. Based on the measured speed-of-sound data, isobaric ideal-gas heat capacities were determined with an expanded relative uncertainty of 0.1 %. In comparing the determined  $c_p^0$  values with estimated values reported earlier, deviations on the order of several percent were found beyond the uncertainty. Furthermore, a new temperature correlation function for  $c_p^0$  for HFO-1234yf was developed, which reproduces the  $c_p^0$  values determined in this work within a relative difference of 0.15 %. The new  $c_p^0$  function can be used over the measurement range, contributing to an improvement of a new equation of state for HFO-1234yf.

## References

1. O.J. Nielsen, M.S. Javade, M.P. Sulbaek Andersen, M.D. Hurley, T.J. Wallington, R. Singh, Chem. Phys. Lett. **439**, 18 (2007)
2. T. Hozumi, T. Koga, H. Sato, K. Watanabe, Int. J. Thermophys. **14**, 739 (1993)
3. T. Hozumi, H. Sato, K. Watanabe, J. Chem. Eng. Data **39**, 493 (1994)
4. T. Hozumi, H. Sato, K. Watanabe, Int. J. Thermophys. **17**, 587 (1996)
5. T. Hozumi, H. Sato, K. Watanabe, J. Chem. Eng. Data **41**, 1187 (1996)
6. T. Hozumi, H. Sato, K. Watanabe, J. Chem. Eng. Data **42**, 541 (1997)
7. K. Ogawa, T. Kojima, H. Sato, J. Chem. Eng. Data **46**, 1082 (2001)
8. H. Preston-Thomas, Metrologia **27**, 3 (1990)
9. M.R. Moldover, J.P.M. Trusler, T.J. Edwards, J.B. Mehl, R.S. Davis, J. Res. Natl. Bur. Stand. (U.S.) **93**, 85 (1988)
10. J.B. Mehl, M.R. Moldover, J. Chem. Phys. **74**, 4062 (1981)
11. M.B. Ewing, M.L. McGrashan, J.P.M. Trusler, Metrologia **22**, 93 (1986)
12. J.B. Mehl, J. Acoust. Soc. Am. **71**, 1109 (1982)
13. International Organization for Standardization (ISO), *Guide to the Expression of Uncertainty in Measurement* (ISO, Geneva, Switzerland, 1993), p. 101
14. R. Akasaka, K. Tanaka, Y. Higashi, Int. J. Refrig. **33**, 52 (2010)
15. M.L. Huber, A. Laesecke, R.A. Perkins, Ind. Eng. Chem. Res. **42**, 3163 (2003)
16. K.G. Joback, R.C. Reid, Chem. Eng. Commun. **57**, 233 (1987)
17. Y. Yoneda, Bull. Chem. Soc. Jpn. **52**, 1297 (1979)
18. T.J. Leck, in *Proceedings 3rd IIR Conference on Thermophysical Properties and Transfer Processes of Refrigerants* (Boulder, CO, 2009)
19. K. Tanaka, Y. Higashi, Int. J. Refrig. **33**, 474 (2010)